BENZIMIDAZOLE BASED FLUORESCENT CHEMOSENSORS AND THEIR PROPERTIES AS MOLECULAR LOGIC GATES

A Thesis

submitted in partial fulfillment of the requirements

for the award of the degree of

MASTER OF SCIENCE

IN

CHEMISTRY

By

MAITRI BHUTANI

Registration No. 300902010

Supervisor

DR. SUSHEEL MITTAL

Co-Supervisor

DR. VIJAY LUXAMI

SCHOOL OF CHEMISTRY AND BIOCHEMISTRY

THAPAR UNIVERSITY, PATIALA

JULY, 2011

DEDICATED TO MY PARENTS.....

Certificate

This is to certify that the project entitled **"Benzimidazole Based Fluorescent Chemosensors and Their Properties As Molecular Logic Gates"** being submitted by Maitri Bhutani, Roll No. 300902010 in partial fulfillment of the requirements for the award of degree of Master of Science in School of Chemistry and Biochemistry, Thapar University, Patiala, is a bonafide work carried out under my supervision and guidance. The report has not been submitted for the award of any other degree or certificate in this or any other university.

Susheel Mittal 14/7

Dr. Susheel Mittal
Supervisor and Head
SCBC
Thapar University, Patiala

Vijay Luxami 14-07-2011

Dr. Vijay Luxami
Co-supervisor
SCBC
Thpar University, Patiala

Dr. S. K. Mohapatra
Dean, Academic Affairs
Thapar University, Patiala

Candidate's Declaration

I hereby declare that the work which is being presented in the dissertation entitled **"Benzimidazole Based Fluorescent Chemosensors and Their Properties As Molecular Logic Gates"** in partial fulfillment of the requirements for the award of the degree of master of science in Chemistry, School of Chemistry and Biochemistry, Thapar University, Patiala is an authentic record of my own work during a period of six months from January 2011 to July 2011, under the supervision of Dr. Susheel Mittal, Senior Professor and Head, and co supervisor Dr. Vijay Luxami, Lecturer, School of Chemistry and Biochemistry, Thapar University, Patiala. The report has not been submitted for the award of any other degree or certificate in this or any other university.

Maitri

Maitri Bhutani

Place: Patiala

Date: 14-07-11

This is to certify that the above statement given by the candidate is correct and true to the best of our knowledge.

Susheel Mittal 14/7/11

Dr. Susheel Mittal
Supervisor and Head
SCBC, TU
Patiala

Vijay Luxami 14-07-2011

Dr. Vijay Luxami
Co-Supervisor
SCBC, TU
Patiala

Acknowledgement

In pursuit of this academic endeavor, I feel that I have been singularly fortunate because inspiration, guidance, direction, co-operation, love and care- all come in my way in abundance and it seems almost an impossible task for me to acknowledge the same in adequate term.

My wholehearted indebtness goes to my erudite guide, **Dr. Susheel Mittal**, Senior Professor and **Head**, and co guide **Dr. Vijay Luxami,** Lecturer, School of Chemistry and Biochemistry, Thapar University, Patiala, for their support and patience. Their invaluable assistance and precious guidance helped me in executing this arduous task from its conception to its completion.

I thank Ms. Karamjeet Kaur, Ms. Nidhi Gupta and Mr. Jasminder Singh, research scholars for their kind cooperation during the project work.

Life at Thapar University would be unforgettable for me throughout my life because I was blessed to spend it with friends like Mandeep, Tajbir, Deepshikha, Karnika and Banpreet. I thank them all for their great company.

Words fail me to express my thanks to my family for their selfless sacrifice, encouragement and heart full blessings that continue to enlighten my life.

Above all I thank almighty God for blessing me with strength and wisdom to complete this project successfully.

Maitri

Maitri Bhutani

CONTENTS

INTRODUCTION & REVIEW OF LITERATURE

Excited- state intramolecular proton transfer (ESIPT) represents a fundamental photophysical process that occurs in a wide range of fluorophores containing an intramolecular hydrogen bond.[1] It occurs in organic bi-functional molecules that contain both hydrogen atom donors (eg. –OH, -NH_2, etc) and acceptors (=N-, >C=O, etc) groups in close proximity.[2] It is basically a photo-tautomerization, i.e, enol to keto transformation in the excited state via an intramolecular hydrogen bond involving the transfer of hydroxyl proton to the electronegative atom, which occurs extremely fast in the sub-picosecond time scale.[3] Proton takes 60 fs to arrive at its tautomer equilibrium position.[4] These reactions are very rapid even at low temperature.[5] The extreme speed is presumably due to the fact that the process involves very slight movement of a light hydrogen atom.[2] The phototautomer formed emits light and thermally equilibrates back to the ground state with the proton bound to its original atom.[6] Energetically the transfer of a normal molecule to its tautomer form is feasible in the S_1 state.[2] This process gives rise to the transient chemical change from enol to keto tautomer, leading to the transient alternation of the electronic properties such as electron density distribution, energies of electronic states, and dipole moments etc.[7]

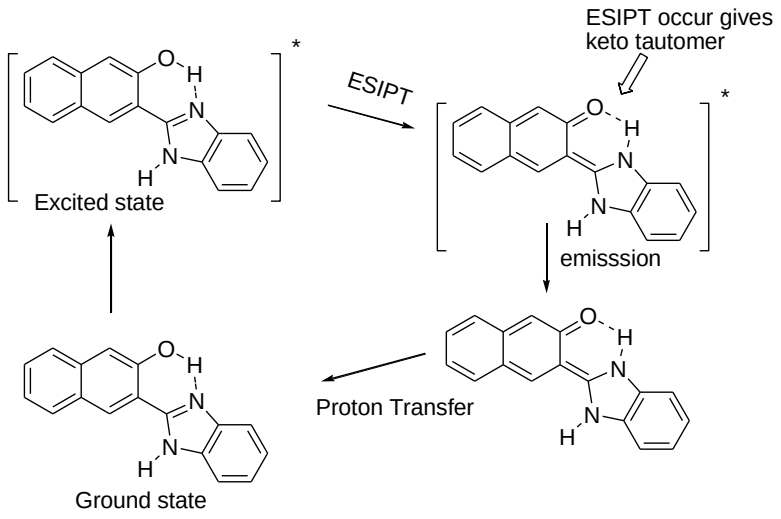

Figure 1

Since the formed phototautomer is only more stable in the excited state but not the ground state, the observed Stokes shift of the fluorescence emission is unusually large with values ranging from 100 to 500 nm.[8] Molecules undergoing ESIPT exhibit dual emission, with the normal one bearing a mirror image relation to the absorption spectrum, arising from an excited species similar in geometry to that in the ground state while the Stokes' shifted emission originates from a tautomer formed in the in the excited electronic state (**figure 1**). The normal and the tautomer excited state emissions depend crucially on the conformation of the molecule, the polarity and hydrogen bonding ability of the solvent, and the temperature.[9-12] In the strongly hydrogen-bonding aqueous medium intermolecular hydrogen bonding favors normal emission.[13] The overall fluorescence emission spectrum depends on the nature of both the ground and excited state of the molecule and is often strongly influenced by the pH as well as the hydrogen-bonding ability and polarity of the solvent.[14, 15]

The efficiency of the ESIPT process is influenced not only by the solvent polarity but also by the pK value of the proton, which is shifted in the excited state. With increasing pK, the thermodynamics of the excited-state proton transfer become less favorable, resulting in an increased normal emission band.[16-18] Therefore, the pK value of the probe should be as low as possible, but still sufficiently high to guarantee protonation of the ground-state species at the pH at which the probe is used.[6]

ESIPT can be observed in a wide range of molecules and has led to various applications in the form of laser dyes,[19,20] high energy radiation detectors,[21-23] UV photostabilizers,[24,25] or fluorescent probes.[26-28] The emission of ESIPT molecules is also responsive toward metal coordination, a property that is of interest for the development of cation sensitive ratiometric fluorescent probes.[29] For such applications, the strong environmental dependence of the emission is undesirable because the probe should only reflect changes in the metal concentration.[6] There are only the few molecules which exhibit ESIPT phenomenon viz. benzimidazole,[2] benzoxazole,[5,30] and benzothiazole (**1-4**) based moieties.

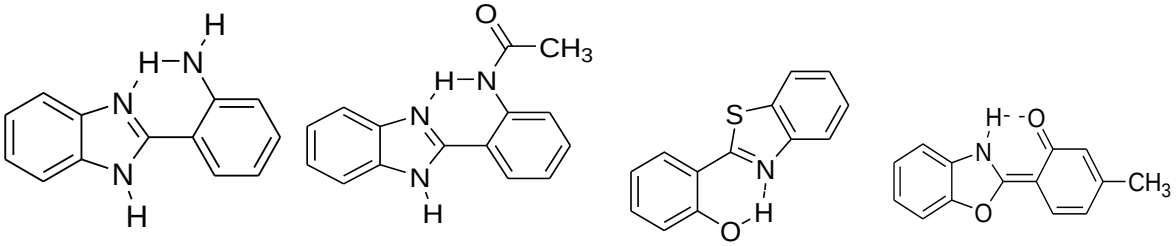

1 **2** **3** **4**

As ESIPT molecules exhibits two emission bands –one due to normal emission and other due to excited state emission, so these molecules in the presence of analyte showed new emission channels. The new emission channel can either be blue shifted or red shifted with respect to normal and excited emissions. Thus, emission at one chanel is switched "OFF" and emission at other channel is switched "ON". This switching ON-OFF of fluorescence provides the opportunity for the ratiometric sensing.

In literature, most of the available metal ion sensors detect the analyte concentration by either increase or decrease in the emission intensity. But the emission intensity is also dependent on many other factors, such as emission collection efficiency, environment around the sensor, sensor concentration, and optical path length and illumination intensity.[31] Therefore, it is desirable to eliminate the effect of these factors by using a ratiometric sensor. This kind of sensor exhibits a spectral shift upon reaction or binding to the analyte of interests, and the ratio of emission intensities between the ligand and its complex can be used to evaluate analyte concentration.[32] They determine the free metal concentration directly from the ratio of the emission intensities at two wavelengths. The major restriction on the design of this type of sensor is from the necessity for a spectral-shift upon binding metal ions. These chemosensors are based on a "switching on/off" mechanism, such that the fluorescent output is quenched in the absence, and restored upon binding of the analyte. Due to the linear relationship between fluorescence intensity and analyte concentration, such probes can principally be used for quantitative measurements.[4]

Lippard et al,[33-35] Tsien,[34,35] O'Halloran,[36] Kennedy,[37] and Gee[38] and co-workers have recently introduced a new generation of sensors based on fluorescein and rhodamine chromophores conjugated to picolylamines, aminocarboxylate, and cyclen chelating groups. The prime advantage of these sensors lies in the use of bright and relatively longer wavelength absorption/emission chromophores.[39]

The fluorescence spectrum of **5** exhibits emission band with a maximum at 483 nm when excited at 360 nm. Selective and large fluorescent enhancements were observed upon addition of Zn^{2+} (22 fold) to the solution of **5**. Addition of Zn^{2+} ion to the aqueous solution (CH_3CN/0.5M HEPES, pH=7.4, 50:50) caused a red shift to 514 nm.[40]

The fluorophore **6** behaves as an ratiometric zinc sensor. Under stimulated physiological conditions (50 mM aqueous PIPES buffer, 100 mM KCl, pH 7.0), **6** exhibits visible absorption and emission maximum at 514 and 540 nm, respectively. Zinc coordination prompts a hygroscopic shift of the emission band to 523 nm.[41]

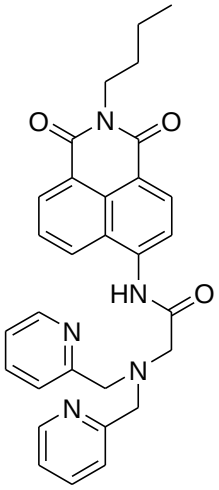

5

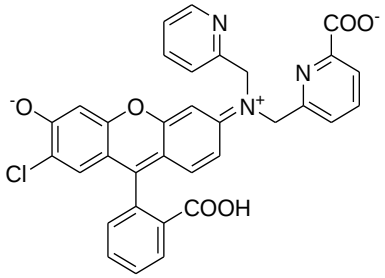

6

Another example of ratiometric sensor for zinc is **7.** The λ_{ex} for **7** is 410 nm and it gives the emission peak at 484 nm. Incremental addition of Zn^{2+} result in a 21 nm bathochromic shift of the $\lambda_{max\text{-}emission}$ of **7** and now it appears at 505 nm. This shift is solvent-dependent and is minimized in solvent systems containing increasing amounts of water.[39]

2-(hydroxymethyl)-4-methyl-6-((quinolinyl-8-imino)methyl) phenol (HMQP)] **8** based ratiometric sensor used for detection of zinc. The compound **8** on excitation at 455 nm, exhibits the emission maximum at 515 nm with a low quantum yield at room temperature in Tris-HCl (50 mM, pH = 7.54), THF-H_2O (9:1 v/v). Upon addition of 0.5 equivalents of Zn^{2+}, the fluorescence intensity of **8** increases by 14 fold, the emission maximum shifts from 515 to 565 nm. The emission maximum of **8** was shifted to 565 nm with significant color change from colorless to yellow. When

Zn^{2+} was introduced to **8**, the intramolecular H-bond of **8** is broken which prohibits intramolecular electron transfer process and then enhances fluorescence emission.[42]

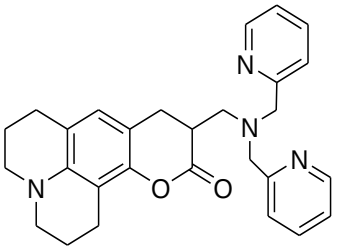

7

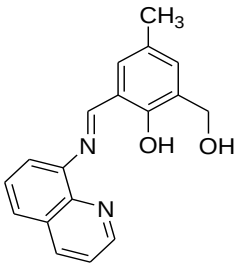

8

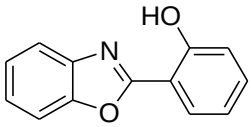

9

The 2-(2'-hydroxyphenyl)-benzoxazole (HPBO) **9** undergo structural transformation between the enol and keto tautomers and thus exhibit ESIPT phenomenon. The ESIPT of HPBO results in a large Stokes shift ranging from 100 to 500 nm. HPBO chelate with the Zn^{2+} ions. And during the process of the coordination with zinc ion, the phenol group in the HPBO is deprotonated, and the generated phenolate anion acts as a donor in the zinc complex. Through the complexation with zinc ions, the ESIPT process is efficiently disrupted and a blue shifted emission is detected from the zinc complex. Because of these specific characteristics, HPBO-containing compounds are considered to be functional materials for sensors. The compound **10** containing fluorene vinylene moiety in the structural centre and HPBO derivatives as the end group behaves as Zn^{2+} sensor. Zn complex of **10** gives emission peak at 500 nm when excited at 387 nm.[43]

The chemosensor **11** shows strong fluorescence in acidic and neutral solutions. Upon excitation of solution of **11** (100 mM HEPES, pH 7.4) at 513 nm, an emission spectrum with a maximum at 543 nm was observed. Coordination of Zn^{2+} to **11** led to striking changes in the emission color. Upon addition of Zn^{2+} to **11**, produces a fluorescence spectrum centered at 558 nm.[44]

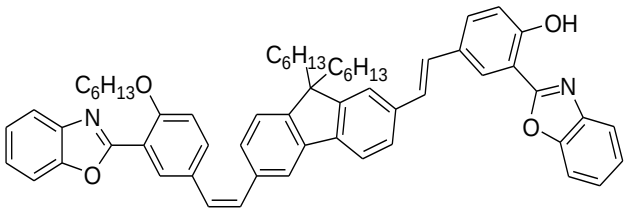

10

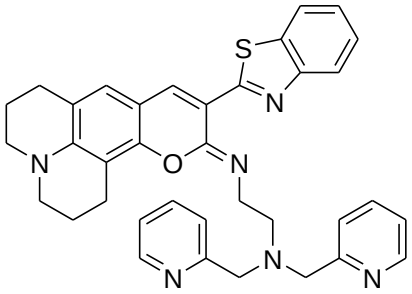

11

The molecule or the fluorescent probes demonstrates "on" or "off" switching of the fluorescence signal meaning "1" or "0" respectively as output, in response to the addition "1" or non-addition "0" of the input chemicals and hence can be used for the construction of molecular logic gates. Most of the molecular systems express a single logic function by a combination of a certain two chemical inputs.[45] Metal cations are often used as the input chemicals for reconfiguration of the logic functions, because the emission behavior of the fluorophores usually depends strongly on the nature of metal cations. A molecular logic gate is a molecule that performs a logical operation on one or more logic inputs and produces a single logic output. Molecular logic gates work with input signals based on chemical processes and with output signals based on spectroscopy. They function as switches whose output (0 or 1) depends on input conditions.[46] Any chemical system that can exist in two quasi-stable states of different chemical or physical properties may be regarded as a molecular logic gate, provided there are some physical or chemical stimuli that can (reversibly) change the state of the system.

<u>One Input Logic Gates</u>

There are four possible combinations of input and output values for one-input one-output logic gates. The four gates are: PASS 0, PASS 1, YES and NOT. The PASS 0 and PASS 1 gates yield 0 and 1 output, respectively, independently of the input value. The YES gate follows the input value to the output (**table 1**). The NOT gate performs inversion of the input data. It changes one logic level into the opposite : logic 0 is converted into logic 1 and vice versa.[46]

Table 1: Truth Table For Single Input Logic Gate

output / input	PASS 0	YES	NOT	PASS 1
	-	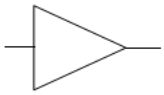	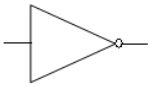	-
0	0	0	1	1
1	0	1	0	1

Multiple Input logic gates

There are 16 various combinations of input and output signals for two-input logic gates, 8 of which are commonly used: basic OR, AND, and XOR, and gates concatenated with NOT, NOR, AND and XNOR. INHIBIT (INH) and NINH gates are also regarded as simple logic gates (**table 2**). The OR gate is one of the basic gates from which all other functions can be constructed. The OR gate produces high output when any of the inputs is in the high state, and the output is low when all the inputs are in the low state. Therefore, the gate detects any high state at any of the inputs. It computes the logic sum of input variables, that is, it performs the union operation.

Table 2: Truth Table For Two Input Logic Gates

output / input		OR	AND	XOR	INH	NOR	NAND	XNOR
		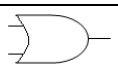	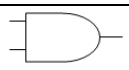	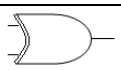	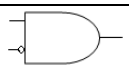	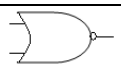	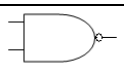	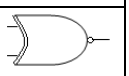
0	0	0	0	0	0	1	1	1
0	1	1	0	1	1	0	1	0
1	0	1	0	1	0	0	1	0
1	1	1	1	0	0	0	0	1

The AND gate is another of the principal logic gates, it has two or more inputs and one output. The AND gate produces high output (logical 1) only when all the inputs are in the high state. If any one of the inputs is in the low state, the output is also low. The main role of gate is to determine if the input signals are simultaneously true. It performs the intersection operation or computes the logic product of input variables.

The XOR gate is not a principal gate, but it is actually formed by a combination of the gates described above. Due to its fundamental importance in numerous applications, this gate is treated as a basic logic element, and it has been assigned a unique symbol. The XOR gate yields the high output when two input values are different, but yields low output when the input signals are identical. Main application of the XOR gate is binary half-adder, simple electronic circuit enabling transition from Boolean logic to arithmetic. The whole family of logic gates is formed by concatenation of OR, AND, and XOR gates with NOT gate, which can be connected to the input or output of any of the above gates.[46]

Combinatorial logic gates

A circuit comprising connected logic gates, devoid of feedback loops (memory), is a combinatorial logic gate, a device whose signal is a unique Boolean function of input variables. The most important are binary half-adder and half-substractor, and full adder.[47] These circuits enable arithmetic operations on bits of information in binary fashion. The half-adder is a device composed of two gates: AND and XOR. It has two inputs (two bits to be added) and two outputs (sum and carry). Half-substractor is a related circuit (the only difference lies in one NOT gate at input), which performs a reverse operation: it substracts the value of one bit from the other, yielding the bit of difference and a bit of borrow. Full adder consists of two half-adders and OR gate. The circuit performs full addition of three bits, yielding two-bit results. Similarly, full substractor can substract three one-bit numbers, yielding two-bit binary result.[46]

The first logic gate has emerged from fluorescent probes based on molecular recognition of target molecules.[48-51] These gates and other devices were controlled exclusively by chemical signals, while the output was observed as changes in fluorescence.[46]

The probe **12** functions as an OR logic gate. The OR gate, which computes the logic sum of two input variables, is the easiest to be implemented in molecular

systems. **12** are based on PET phenomenon. The tricarboxylate receptor part can successfully bind magnesium and calcium ions. This nonselectivity constitutes the basis of OR operation. On ion binding, the electronic structure of the molecule is rearranged, and the fluorescence of the fluorophore is switched on.[52]

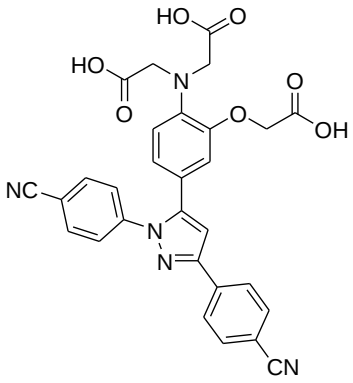

12

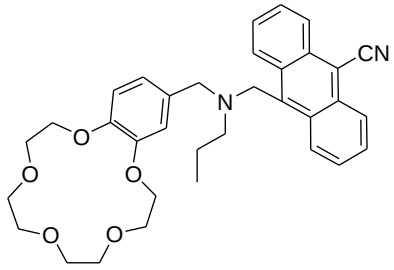

13

Most of the molecular AND logic gates are based on ditopic receptors and a fluorescent unit linked covalently with both receptors. In contrast to the OR gate, fluorescence should be switched on when both receptors bind corresponding substrates.[53] **13** makes AND logic gate. The gate consists of three structural elements : the cyanoanthryl fluorophore, azacrown cation receptor, and the tertiary amino group (proton acceptor). Upon excitation of the fluorophore, PET processes from the azacrown and tertiary amine efficiently quench the fluorescence. Binding of sodium within the azacrown does not influence the luminescence of the compound as PET from amine can efficiently quench the fluorescence. Only simultaneous binding of two substrates to the receptors (sodium cations and protons) prohibits PET and switches the fluorescence on.[46]

RESULTS & DISCUSSION

In the present work, new ESIPT based fluorescent probes **1-2** have been investigated towards different metal ions and some tetrabutyl-ammonium anions. The studies shows that the probes **1-2** exhibits the differential behavior towards Cu^{2+} and Zn^{2+} ions and other metals ions does not interfere in their estimation. In case of various anions, only tetrabutyl-ammonium fluoride showed the selective behavior. The studies were further extended to evaluate the effect of pH on the ESIPT behavior. The differential behavior of cations and anions were elaborated for the molecular logic functions.

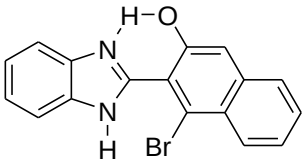

1

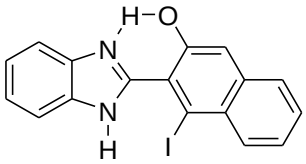

2

Photophysical studies of probes 1-2

The photophysical behavior of probes **1-2** has been studied through UV-Vis spectroscopy and fluorescence spectroscopy.

UV-Vis behaviour of probes 1-2

Chemosensors **1** and **2** (20 µM, CH_3CN) show the absorption bands at λ_{max} 282 (ε 26000), 312 (ε 34000), 330 (ε 34000) and 360 (ε 6500) nm. In the preliminary UV-Vis studies, chemosensors **1** and **2** did not show any visual colour and spectrophotometric changes with different anions, except fluoride ions and except Cu^{2+} and Zn^{2+} amongst metal ions. A visible color change from colourless to pale yellow is observed for Cu^{2+}, Zn^{2+} and F^- due to discrete but small increase in absorption between 400 nm - 450 nm.

Fluorescence behavior of Probe 1 towards metal ions:

The Probe **1,** on excitation at 330 nm (10^{-5} M, CH_3CN) exhibited the emission maximum at 580 nm (strong band) and normal emission at 397 nm (weak band). On addition of different metal ions, *viz.* Li^+, Na^+, K^+, Mg^{2+}, Ca^{2+}, Ba^{2+}, Cr^{3+}, Fe^{2+}, Co^{2+}, Ni^{2+}, Hg^{2+}, Cd^{2+}, Ag^+ and Pb^{2+}, to the solution of probe **1**, there is no significant change in its fluorescence spectrum except in case of addition of Cu^{2+} and Zn^{2+} ions. The emission band at 580 nm is completely quenched in the presence of Cu^{2+} ions where as in case of addition of Zn^{2+} ions, the emission band at 580 nm is quenched along with the formation of new emission band at 494 nm. However, no change is observed for the band at 397 nm.

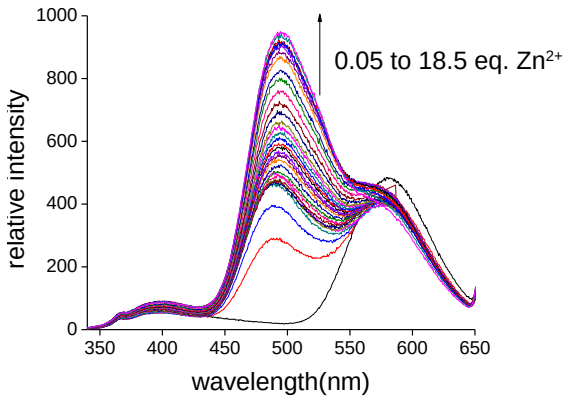

Figure 1: Effect of incremental addition of Zn^{2+} on probe **1** (CH_3CN, 10^{-5} M).

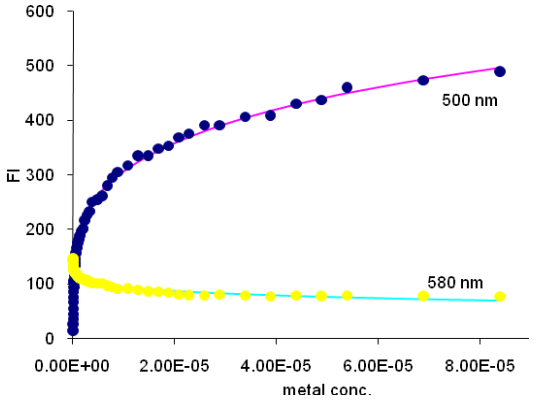

Figure 2: Spectral fitting of Zn^{2+} titration curve of probe **1** (λ_{ex} 330 nm) at 500 nm and 580 nm.

In order to evaluate the complete structural behavior of probe **1** towards Cu^{2+} and Zn^{2+} ions, the fluorescence titration of probe **1** was performed at different concentrations of metal ions. On addition of 0.05 equivalent of Zn^{2+} ion to the solution of probe **1**, the new emission band at 494 nm appeared. On incremental addition of the reagent, the peak at 580 nm gets quenched and it achieves the plateau after 18 equivalents (Figure 1). The spectral curve fitting of the data shows the formation of ML and ML_2 stoichiometric species, with stability constant log βML = 5.63 ± 0.15 and βML_2 = 13.15 ± 0.2 (Figure 2).

In case of incremental addition of Cu^{2+} ions, the emission band at 580 nm was completely quenched and achieved the plateau after 2 equivalents (Figure 3). The spectral curve fitting of the data shows the formation of M_2L stoichiometric species, with stability constant log β = 16.11 ± 0.5 (Figure 4).

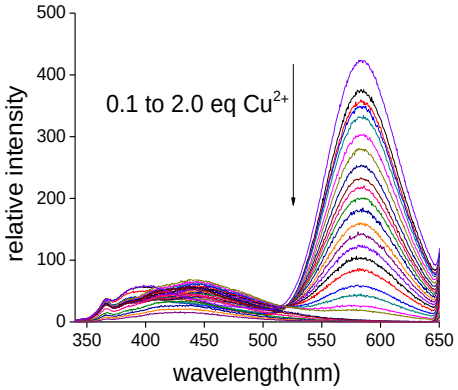

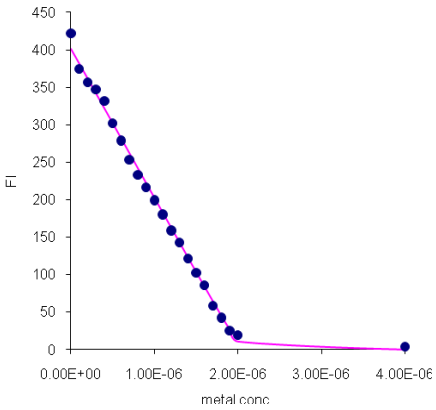

Figure 3: Effect of incremental addition of Cu^{2+} on probe **1** (CH_3CN, 10^{-5} M).

Figure 4: Spectral fitting of Cu^{2+} titration curve of probe **1** (λ_{ex} 330 nm) at 580 nm.

Thus, the two metals ions showed the differential emission behavior. Further, it was further evaluated whether this is in actual the metal ion behavior responsible for the differential emission behavior or the effect of charge on the metal ions. So, the studies were further extended to evaluate the effect of $HClO_4$ on the fluorescence behavior of probe **1**. Upon addition of $HClO_4$ to the solution of probe **1**, the emission maximum at 580 nm was quenched along with the formation of new emission band at 445 nm. Incremental addition leads to increase in intensity of the peak at 445 nm and decrease in intensity of the peak at 580 nm and it achieved the plateau after 26 equivalents (Figure 5). The spectral curve fitting of the data shows the formation of M_2L stoichiometric species with stability constant log βM_2L = 12.27 +0.07 (Figure 6).

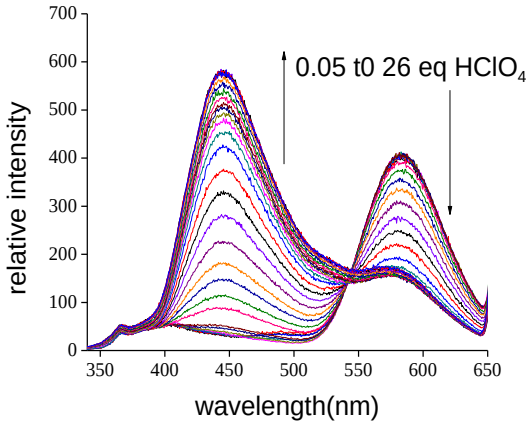

Figure 5: Effect of incremental addition of $HClO_4$ on probe **1** (CH_3CN, 10^{-5} M).

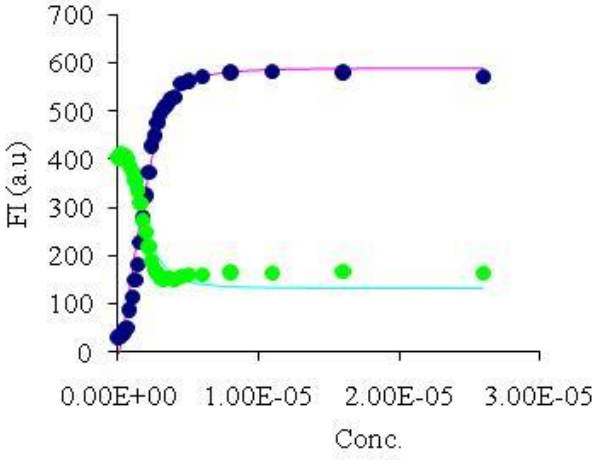

Figure 6: Spectral fitting of $HClO_4$ titration curve of probe **1** (λ_{ex} 330 nm) at 445 nm and 580 nm.

Photophysical behavior of 1 in presence of anions

On addition of different anioins, *viz*. Cl^-, Br^-, F^-, I^-, CN^-, CH_3COO^-, HSO_4^-, ClO_4^- to the solution of probe **1**, there is no significant change in its fluorescence spectrum except in the case of addition of F^- ions. In order to evaluate the complete structural behavior of probe **1** towards F^- ions, the fluorescence titration of probe **1** was performed at different concentrations of the anion. Upon addition of 1 equivalent of F^- ions (as tetrabutylammoniumfluoride or TBAF), a new emission peak at 503 nm is observed along with the emission peak at 580 nm. Further addition leads to an increase in the intensity of the peak at 503 nm and quenching of the emission peak at 580 nm and it achieves the plateau after 6.8 equivalents (Figure 7).

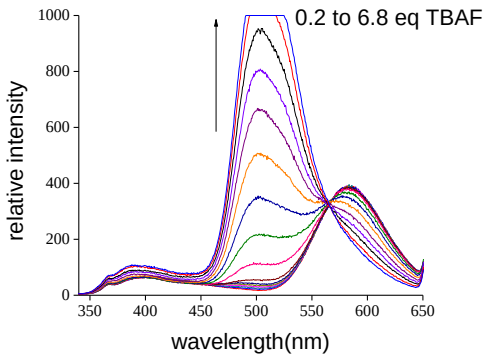

Figure 7: Effect of incremental addition of TBAF on probe **1** (CH_3CN, 10^{-5} M).

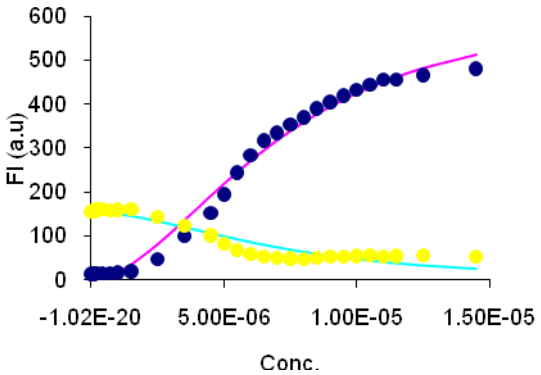

Figure 8: Spectral fitting of TBAF titration curve of probe **1** (λ_{ex} 330 nm) at 503 nm and 580 nm.

The spectral curve fitting of the data shows the formation of LF_2 stoichiometric species with stability constant log βLF_2 = 10.47 $\pm$ 0.15 (Figure 8).

Fluorescence behavior of Probe 2 towards metal ions:

The Probe **2,** on excitation at 330 nm (10^{-5} M, CH_3CN) exhibited the emission maximum at 580 nm (strong band) and normal emission at 395 nm (weak band). The difference in the emission spectra of probe **1** and **2** lies in the intensity of the emission peak at 580 nm, the intensity of probe **1** being 3 times greater than that of probe **2**. On addition of different metal ions, *viz.* Li^+, Na^+, K^+, Mg^{2+}, Ca^{2+}, Ba^{2+}, Cr^{3+}, Fe^{2+}, Co^{2+}, Ni^{2+}, Hg^{2+}, Cd^{2+}, Ag^+ and Pb^{2+}, to solution of probe **2**, there is no significant change in its fluorescence spectrum except in case of addition of Cu^{2+} and Zn^{2+} ions. The emission band at 580 nm is completely quenched in the presence of Cu^{2+} ions where as in case of addition of Zn^{2+} ions, the emission band at 580 nm is quenched along with the formation of new emission band at 494 nm.

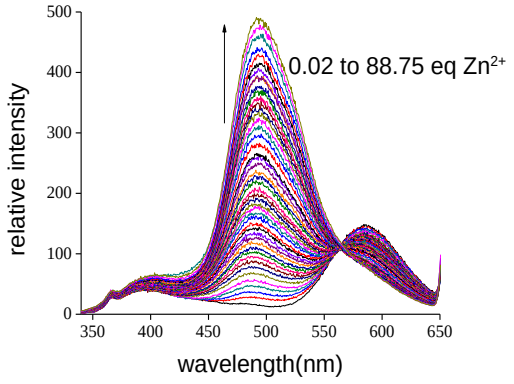

Figure 9: Effect of incremental addition of Zn^{2+} on probe **2** (CH_3CN, 10^{-5} M).

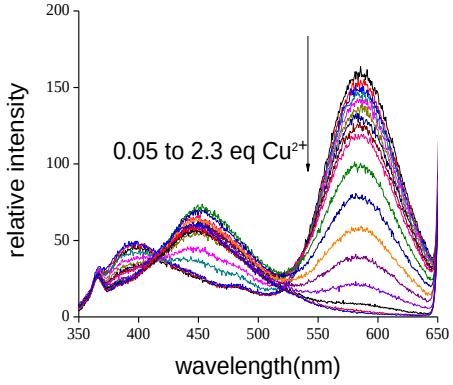

Figure 10: Effect of incremental addition Cu^{2+} on probe **2** (CH_3CN, 10^{-5} M).

In order to evaluate the complete structural behavior of probe **2** towards Cu^{2+} and Zn^{2+} ions, the fluorescence titration of probe **2** was performed at different concentrations of metal ions. Upon addition of 0.02 equivalents of Zn^{2+} ions, a new peak at 494 nm is observed along with the peak at 580 nm. Incremental addition of

Zn^{2+} ions leads to an increase in intensity of the peak at 494 nm and the peak at 580 nm gets quenched. The plateau is achieved after 88 equivalents (Figure 9).

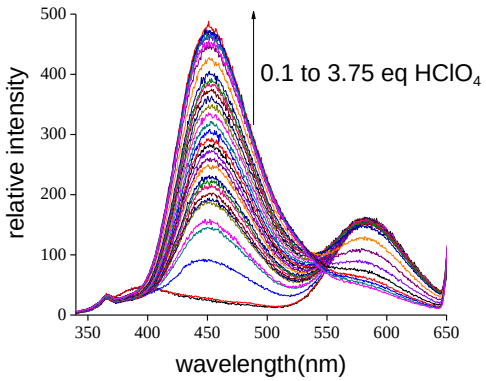

Figure 11: Effect of incremental addition of $HClO_4$ on probe **2** (CH_3CN, 10^{-5} M).

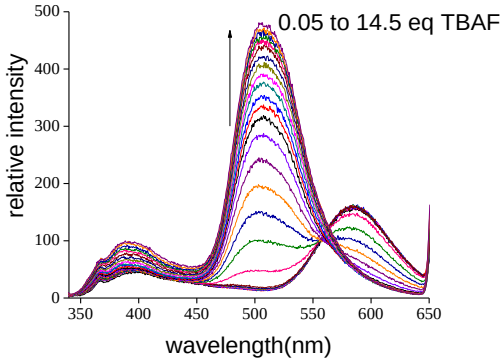

Figure 12: Effect of incremental addition of TBAF on probe **2** (CH_3CN, 10^{-5} M).

In case of incremental addition of Cu^{2+} ions, the emission band at 580 nm was completely quenched and achieved the plateau after 2 equivalents (Figure 10). Upon addition of 0.2 equivalents of $HClO_4$ to the solution of probe **2**, a new peak at 452 nm was observed along with the peak at 580 nm. Its incremental addition leads to increase in intensity of the peak at 452 nm and the peak at 580 nm gets quenched. It achieves the plateau after 3.75 equivalents (Figure 11).

Upon addition of 1 equivalent of TBAF to the solution of probe **2**, a new peak at 507 nm is observed along with the peak at 580 nm. Further addition leads to increase in intensity of the peak at 507 nm and decrease in intensity of the peak at 580 nm and the plateau is achieved after 14.5 equivalents (Figure 12).

The fluorescence behavior of two probes **1-2** shows that probe **1** is more sensitive towards analyte but probe **2** is more selective for the analytes. This behavior can be explained on basis of size of halide ion present on the probes. Probe **2** having large sized iodide ions shows the more selectivity for the ions by restricting the ESIPT phenomenon than probe **1**.

Effect of pH on Probe 1-2:

Effect of pH on fluorescence behavior of probes **1-2** has been evaluated by varying the pH on addition of acid and base to the 10 µM (4:1 :: CH_3CN: H_2O) solution. The emission spectrum of Probe **1** (10^{-5} M, 4:1:; CH_3CN: H_2O) on excitation at 330 nm, exhibits emission maximum at 580 nm and 390 nm. On incremental decreasing pH (by adding HCl), the fluorescence intensity at 580 nm remained unaffected. Upon decreasing the pH up to 4.0, emission band at 390 nm gets increased and on further decreasing the pH upto 2.0, this band remains unaffected but there is formation of new emission band at 425 nm which achieves the plateau at pH 1.8 (Figure 13).

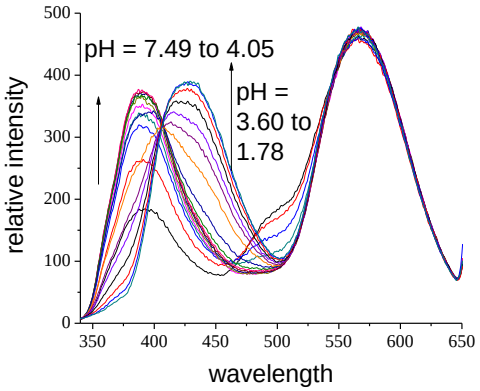

Figure 13: Effect of acidic pH (7.5-1.7) on fluorescence behavior of probe **1**.

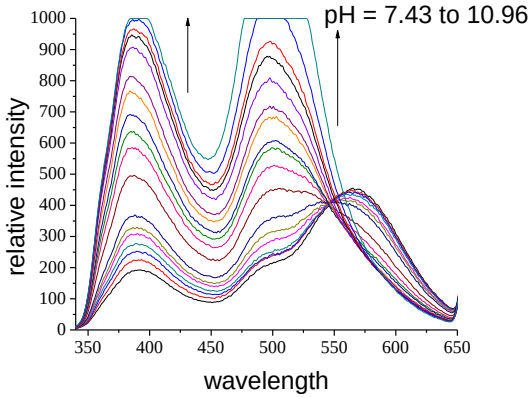

Figure 14: Effect of basic pH (7.5-11.0) on fluorescence behavior of probe **1**.

On incremental increasing pH (by adding NaOH), the fluorescence intensity at 390 nm gets enhanced while the fluorescence intensity at 580 nm gets quenched along with the formation of new emission band at 500 nm. The emission intensity at 390 nm and 500 nm went off scale at pH 10.9 (Figure 14). Similarly, the Probe **2** (10^{-5} M, 4:1:; CH_3CN: H_2O) on excitation at 330 nm exhibited emission maximum at 580 nm and 390 nm. On decreasing the pH, the emission band at 580 nm remains unaffected but the emission at 390 nm gets quenched along with the formation of weak emission band at 445 nm (Figure 15).

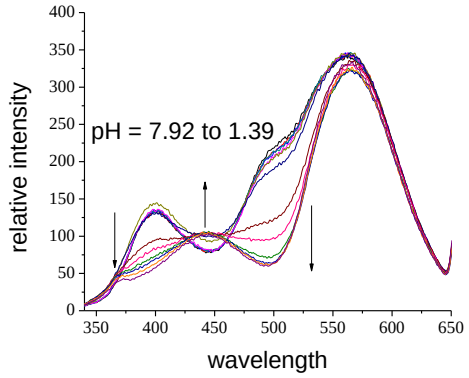

Figure 15: Effect of acidic pH (8-1.3) on fluorescence behavior of probe **2**.

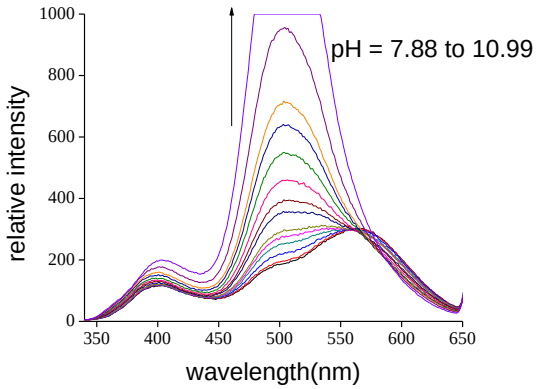

Figure 16: Effect of basic pH (7.8-11.0) on fluorescence behavior of probe **2**.

On incremental increasing pH (by adding NaOH) of probe **2**, the fluorescence intensity at 580 nm and 390 nm remains almost unaffected but there is a formation of new emission band at 500 nm and went off scale at pH 10.9 (Figure 16).

The fluorescence behavior of two probes upon varying the pH showed very different properties. In case of probe **1,** having relatively lighter bromo group, varying the pH, totally inhibits the ESIPT phenomenon (quenched 580 nm) and release the normal emission band at 390 nm and deprotonated emission band at 500 nm. In the case of probe **2,** the bulkier iodo group is not able to inhibit the ESIPT phenomenon completely and thus could not release the normal emission band at 390 nm. This behavior is quite clear from the experimental results, as in case of probe **2,** ESIPT band (580 nm) remains unaffected and only deprotonated emission band at 500 nm is released.

Fluorophore **1** (10 µM CH_3CN) on excitation at 330 nm gave emission maxima at 580 nm and is attributed to ESIPT from phenolic OH to benzimidazole nitrogen. Addition of Zn^{2+}, $HClO_4$ and TBAF leads to quenching of the ESIPT band at 580 nm and gave the new peaks at 494 nm, 445 nm and 503 nm, respectively. With fluorophore **2**, the peaks obtained with Zn^{2+}, $HClO_4$, and TBAF are at 494 nm, 452 nm and 507 nm, respectively. Thus, addition of these analytes to the probes **1-2** opens four new emission channels which is rare in literature. So, simultaneous opening of

new emission channels can provide the opportunity for elaboration of molecular logic gates.

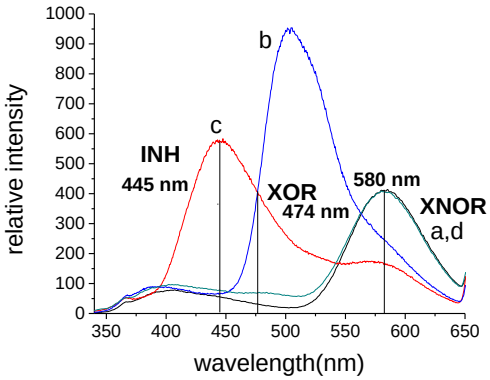

Figure 17: The effect of acid and base on the fluorescence spectrum of fluorophore **1** in CH_3CN: (a) **1** (10 µM), (b) **1** + TBAF (6 equiv.), (c) **1** + $HClO_4$ (26 equiv.) and (d) **1** + $HClO_4$ (4 equiv.) + TBAF (7.5 equiv.).

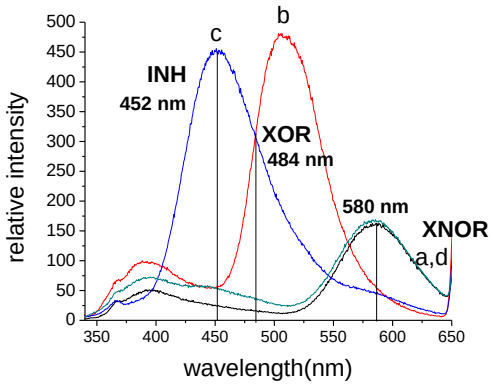

Figure18: The effect of acid and base on the fluorescence spectrum of fluorophore **2** in CH_3CN: (a) **2** (10 µM), (b) **2** + TBAF (14.5 equiv.), (c) **2** + $HClO_4$ (3.75 equiv.) and (d) **2** + $HClO_4$ (2 equiv.) + TBAF (1.95equiv.).

On addition of perchloric acid ($HClO_4$, as acid) (26 equivalents), the emission at 580 nm was completely quenched and a new emission band at 445 nm with hypsochromic shift of 140 nm appeared. On addition of tetrabutylammonium fluoride (TBAF, as base) (7.5 equivalents) to the same solution, the emission at 580 nm reappeared. The addition of TBAF (6.8 equivalents) to the solution of **1** gave a new hypsochromically shifted emission band at 503 nm with concomitant quenching at 580 nm (Figure 17). The emission output of **1** at 503 nm is turned "ON" (output = 1) only in the presence of TBAF as input. For all other circumstances, the output signal is "OFF" (output = 0) (threshold value 180). This output correlates well with XOR logic gate at 474 nm (with TBAF turned "ON"). Similarly, the emission output of **1** at 445 nm is turned "ON" (output = 1) only in the presence of $HClO_4$ as input and for all other circumstances output signal is turned "OFF" (threshold value 200). This output correlates well with INHIBIT logic gate at 445 nm (with $HClO_4$ turned "ON"). Probe **1** on addition of two simultaneous inputs in the form of $HClO_4$ (acid) and TBAF (base) annihilate each other's action and generate the emission at 580 nm. This results

in an XNOR logic gate which is active only if both or neither of inputs are present (Figure 19).

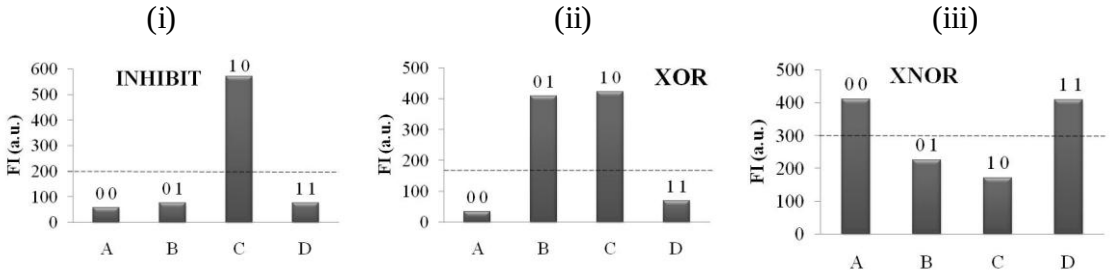

Figure 19: Bar diagram showing (i) INHIBIT logic gate at 445 nm (ii) XOR logic gate at 474 nm (iii) XNOR at 580 nm with probe **1** at different inputs, (A) **1** (10 μM), (B) **1** + TBAF (6 equiv.), (C)**1** + $HClO_4$ (26 equiv.) and (D) **1** + $HClO_4$ (4 equiv.) + TBAF (7.5 equiv.)

Fluorophore **2** (10 μM, CH_3CN) on excitation at 330 nm gave emission maxima at 580 nm and it is attributed to ESIPT from phenolic OH to benzimidazole nitrogen. On addition of perchloric acid ($HClO_4$, as acid) (4 equivalents), the emission at 585 nm was completely quenched and a new emission band at 452 nm appeared. On addition of tetrabutylammonium fluoride (TBAF, as base) (2 equivalents) to the same solution, the emission at 580 nm reappeared. The addition of TBAF (14 equivalents) to the solution of **1** gave a new hypsochromically shifted emission band at 507 nm with concomitant quenching at 580 nm (Figure 18).

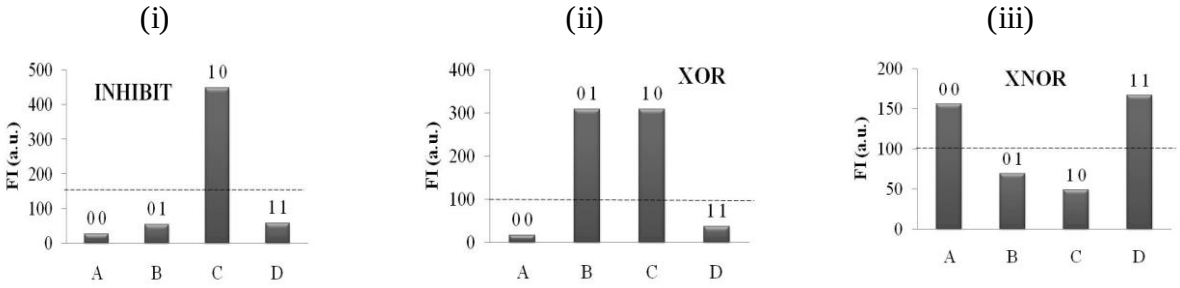

Figure 20: Bar diagram showing (i) INHIBIT logic gate at 452 nm (ii) XOR logic gate at 484 nm (iii) XNOR at 580 nm with probe **2** at different inputs, (A) **2** (10 μM), (B) **2** + TBAF (14 equiv.), (C) **2** + $HClO_4$ (4 equiv.) and (D) **2** + $HClO_4$ (2 equiv.) + TBAF (1.95 equiv.)

The emission output of **2** at 507 nm is turned "ON" (output = 1) only in the presence of TBAF as input. For all other circumstances, the output signal is "OFF" (output = 0) (threshold value 100). This output correlate well with XOR logic gate at 484 nm (with

TBAF turned "ON"). The addition of $HClO_4$ (4 equivalents) to the solution of **2** gave a new hypsochromically shifted emission band at 452 nm with concomitant quenching at 580 nm. Hence, the emission output of **2** at 452 nm is turned "ON" (output = 1) only in the presence of $HClO_4$ as input and for all other circumstances output signal is turned "OFF" (threshold value 180). This output correlate well with INHIBIT logic gate at 452 nm (with $HClO_4$ turned "ON"). Probe **2** on addition of two simultaneous inputs in the form of $HClO_4$ (acid) and TBAF (base) annihilate each other's action and generate the emission at 580 nm. This result in an XNOR logic gate which is active only if both or neither of inputs are present (Figure 20).

Therefore, the probe **1-2** behaves as fluorescent chemosensor for Cu^{2+}, Zn^{2+} and fluoride ions. The differential behavior of these ions provides the opportunity for the elaboration of molecular logic functions as INHIBIT, XOR, XNOR etc.

Experimental

Photophysical studies

All the solvents were of analytical grade and used after distillation. UV-Vis spectroscopy experiments were carried out on Specord 205 by Analytik jena by using slit widths of 1.0 nm and matched quartz cells. The fluorescence experiments were performed on LS55 Perkin Elmer coupled with FL Winlab Software (V 4.00.03) fluorescence spectrophotometer. All absorption and emission scans were saved as ACS II files and further processed in Excel™ to produce all graphs shown. Log β values for anions and metal ion complexation have been determined by analyzing the respective spectral data using an iterative method on multiwavelength data using global analysis programme specfit 32.

The stock solutions of fluorophores **1** and **2** (1 mM) were prepared in CH_3CN. The appropriate amount of aliquot was transfered to measuring flask and solutions were diluted with doubly distilled acetonitrile to get desired solution of fluorophore. The solutions of tetrabutylammonium halides (TBAX) were prepared in doubly distilled acetonitrile. The solution containing fluorophore **1-2** were taken in quartz cell and their fluorescence spectra were recorded. The addition of different concentration of TBA X and $M(ClO_4)_2$ was carried out with a micropipette in aliquots of 1.5-6.0 µl in the same cell and each time the solution was allowed to stand for 3 min before recording the fluorescence spectrum. For interference studies, the solutions of **1** and **2** containing different amounts of TBAF alone or mixtures of TBAF and TBAX were prepared in 10 ml volumetric flasks and their fluorescence spectra were recorded. For, pH titrations, the pH values were lowered and increased by the addition of aqueous HCl and NaOH respectively. All pH measurements were done on pH meter by Equip-Tronics (model number EQ-614).

For metal ion titrations, the solutions of chemosensors **1** and **2** were prepared in CH_3CN-H_2O (4:1) containing 10 mM HEPES buffer. The solutions of metal ions were prepared in distilled water. The solutions of metal ions were added directly into the cuvette containing solution of **1** / **2**. Each time the solution was allowed to stand for 3 min before recording the fluorescence spectrum.

Experimental for Logic gates

Fluorescence spectra were recorded on a Perkin Elmer spectrofluorophotmeter with a 1 cm quartz cell at 25 $\pm$ 1^{o}C. For performing the studies, the solution of fluorophores, tetrabutylammonium hydroxide (TBAF) and perchloric acid ($HClO_4$) were prepared in doubly distilled acetonitrile. The solution containing fluorophore **1** or **2** was taken in quartz cell and their fluorescence spectra were recorded. The addition of different concentrations of TBAF and $HClO_4$ was carried out with a micropipette in aliquots of 1.5-3.0 µl in the same cell and each time the solution was allowed to stand for 3 min before recording the fluorescence spectrum. Titration data were fit with programme Specfit/32, which analyzes multi-wavelength data using an iterative method to obtain the stoichiometries and association constants.

Conclusions

1. Probes **1-2** have been elaborated as selective to differential fluorescent chemosensor for Cu^{2+} and Zn^{2+} ions where Cu^{2+} ions caused only quenching but the Zn^{2+} ions switches "ON" the fluorescence at 500 nm.
2. Probe **1-2** acts as "ON-OFF" molecular switch for Cu^{2+} and "ON-OFF-ON" fluorescent switch for Zn^{2+} ions.
3. Probe **1-2** exhibits the selective ratiometric fluorescent properties for biologically important fluoride ions amongst other anions.
4. Combination of cations and anions turns the fluorescent molecule to work as molecular logic gates.
5. Probe **1-2** has been elaborated as INHIBIT, XOR, XNOR molecular logic circuits.

References

1	Henary, M.M.; Wu, Y.; Cody, J.; Sumalekshmy, S.; Li, J.; Subrata, M.; Fahrni, C.J. *J. Org. Chem.* **2007**, *72*, 4784.
2	Swadeshmukul, S.; Krishnamoorthy, G.; Dogra, S.K. *J. Phys. Chem. A* **2000**, *104*, 476.
3	Abou-Zied, O. K.; Jimenez, R.; Thompson, E. H. Z.; Millar D. P.;Romesberg, F. E. *J. Phys. Chem. A* **2002**, *106*, 3665.
4	Henary, M.M.; Fahrni, C.J. *J. Phys. Chem. A* **2002**, *106*, 5210.
5	Lavtchieva, L.; Enchev, V.; Smedarchina, Z. *J. Phys. Chem.* **1993,** *97*, 306.
6	Fahrni, C.J.; Henary, M.M.; VanDerveer, D.G. *J. Phys. Chem. A* **2002**, *106*, 7655.
7	Seo, J.; Kim, S.; Park, S.Y. *J. Am. Chem. Soc.* **2004**, *126*, 11154.
8	Nagaoka, S.; Kusunoki, J.; Fujibuchi, T.; Hatakenaka, S.; Mukai, K.; Nagashima, U. *J. Photochem. Photobiol. A* **1999**, *122*, 151.
9	Das, K.; Sarkar, N.; Ghosh, A. K.; Majumdar, D.; Nath, D. N.; Bhattacharyya, K. *J. Phys. Chem.* **1994**, *98*, 9126.
10	Das, K.; Sarkar, N.; Majumdar, D.; Bhattacharyya, K. *Chem. Phys. Lett.* **1992**, *198*, 443; **1993**, *204*, 393.
11	Lim, S.-J.; Seo, J.; Park, S. Y. *J. Am. Chem. Soc.*, **2006**, *128*, 14542.
12	Dey, J.; Dogra, S. K. *J. Phys. Chem.* **1994**, *98*, 3638.
13	Sarkar, N.; Das, K.; Das, S.; Datta, A.; Nath, A.; Bhattacharyya, K. *J. Phys. Chem.* **1995**, *99*, 17711.
14	Park, S.; Kwon, O. H.; Lee, Y. S.; Jang, D. J.; Park, S. Y. *J. Phys. Chem. A* **2007**, *111*, 9649.
15	Catala´n, J.; de Paz, J.L.G. *J. Phys. Chem. A* **2008**, *112*, 904.
16	Santra, S.; Dogra, S. K. *Chem. Phys.* **1998**, *226*, 285.
17	Santra, S.; Krishnamoorthy, G.; Dogra, S. K. *Chem. Phys. Lett.* **1999**, *311*, 55.
18	Santra, S.; Krishnamoorthy, G.; Dogra, S. K. *J. Phys. Chem. A* **2000**, *104*, 476.
19	Parthenopoulos, D. A.; McMorrow, D.; Kasha, M. *J. Phys. Chem.***1991**, *95*, 2668.
20	Chou, P. T.; Martinez, M. L.; Clements, J. H. *Chem. Phys. Lett.* **1993**, *204*, 395.
21	Sytnik, A.; Kasha, M. *Radiat. Phys. Chem.* **1993**, *41*, 331.

22	Chou, P. T.; Martinez, M. L. *Radiat. Phys. Chem.* **1993**, *41*, 373.
23	Chung, M. W.; Lin, T. Y.; Hsieh, C. C.; Tang, K. C.; Fu, H.; Chou, P. T.; Yang, S.H.; Chi, Y. *J. Phys. Chem. A* **2010**, *114*, 7886.
24	Keck, J.; Kramer, H. E. A.; Port, H.; Hirsch, T.; Fischer, P.; Rytz, G. *J. Phys. Chem.* **1996**, *100*, 14468.
25	O'Connor, D. B.; Scott, G. W.; Coulter, D. R.; Yavrouian, A. *J. Phys. Chem.* **1991**, *95*, 10252.
26	Sytnik, A.; Kasha, M. *Proc. Natl. Acad. Sci. U.S.A.* **1994**, *91*, 8627.
27	Sytnik, A.; Gormin, D.; Kasha, M. *Proc. Natl. Acad. Sci. U.S.A.* **1994**, *91*, 11968.
28	Sytnik, A.; Del Valle, J. C. *J. Phys. Chem.* **1995**, *99*, 13028.
29	Henary, M. M.; Fahrni, C. J. *J. Phys. Chem. A* **2002**, *106*, 5210.
30	Chen, W.-H.; Xing, Y.; Pang, Y. *Org. Lett.*, **2011**, *13*, 1362.
31	(a) Kawanishi, Y.; Kikuchi, K.; Takakusa, H.; Mizukami, S.; Urano, Y.; Higuchi, T.; Nagano, T. *Angew. Chem., Int. Ed.* **2000**, *39*, 3438. (b)Woodroofe, C. C.; Lippard, S. J. *J. Am. Chem. Soc.* **2003**, *125*, 11458. (c) Liu, Z. P.; Zhang, C. L.; Li, Y. L.; Wu, Z. Y.; Qian, F.; Yang, X. L.; He, W. J.; Gao, X.; Guo, Z. *J. Org. Lett.* **2009**, *11*, 795.
32	(a) Sclafani, J. A.; Maranto, M. T.; Sisk, T. M.; Arman, V. S. A. *Tetrahedron Lett.* **1996**, *37*, 2193. (b) Banthia, S.; Samanta, A. *J. Phys. Chem. B* **2006**, *110*, 6437. (c) Yang, R. H.; Chan, W. H.; Lee, A. W. M.; Xia, P. F.; Zhang, H. K.; Li, K. A. *J. Am. Chem. Soc.* **2003**, *125*, 2884.
33	Pearce, D. A.; Jotterand, N.; Carrico, I. S.; Imperiali, B. *J. Am. Chem. Soc.* **2001**, *123*, 5160.
34	Walkup, G. K.; Burdette, S. C.; Lippard, S. J.; Tsien, R. Y. *J. Am. Chem. Soc.* **2000**, *122*, 5644.
35	Burdette, S. C.; Walkup, G. K.; Springler, B.; Tsien, R. Y.; Lippard, S. J. *J. Am. Chem. Soc.* **2001**, *123*, 7831.
36	Taki, M.; Wolford, J. L.; O'Halloran, T. V. *J. Am. Chem. Soc.* **2004**, *126*, 712.
37	Qian, W.J.; Aspinwall, C. A.; Battiste, M. A.; Kennedy, R. T. *Anal. Chem.* **2000**, *72*, 711.
38	Gee, K. R.; Zhou, Z.-L.; Ton-That, D.; Sensi, S. L.; Weiss, J. H. *CellCalcium* **2002**, *31*, 245.

39	Lim, N.C.; Schuster, J.V.; Porto, M.C.; Tanudra, M.A.; Yao, L.; Freake, H.C.; Bruckner, C. *Inorg. Chem.* **2005**, *44*, 6, 2018.
40	Xu, Z.; Baek, K.H.; Kim, H.N.; Cui, J.; Qian, X.; Spring, D.R.; Shin, I.; Yoon, J. *J. Am. Chem. Soc.* **2010**, *132*, 601.
41	Tomat, E.; Lippard, S.J. *Inorg. Chem*. **2010**, *49*, 9113.
42	Zhou, X.; Yu, B.; Guo, Y.; Tang, X.; Zhang, H.; Liu, W. *Inorg. Chem*. **2010**, *49*, 4002.
43	Tian, Y,; Chen, C.Y.; Yang, C.C.; Young, A.C.; Jang, S.H.; Chen, W.C.; Jen, A.K.Y.*Chem. Mater*. **2008**, *20*, 1977.
44	Komatsu, K.; Urano, Y.; Kojima, H.; Nagano, T. *J. Am. Chem. Soc*. **2007**, *129*, 13447.
45	Nishimura, G.; Ishizumi, K.; Shiraishi, Y.; Hirai, T. *J. Phys. Chem. B* **2006,** *110*, 21596.
46	Szaciłowski, K. *Chem. Rev*. **2008**, *108*, 3481.
47	*The Illustrated Dictionary of Electronics*; Gibilisco S. ed.; McGraw-Hill: New York, 2001.
48	de Ruiter, G.; Tartakovsky, E.; Oded, N.; Boom, M.E. *Angew. Chem*, **2010**, *122*, 173.
49	Inestrosa, E.P.; Montenegro, J.M.; Collado, D.; Suau, R.; Casado, J. *J.Am.Chem.Soc.* **2007**, *111*, 6904
50	Katz, E.; Privman, V. *J. Am. Chem. Soc.* Dx.doi.org/10.1039/B806038J
51	Hosseini, M. W.; Blacker, A. J.; Lehn, J. M. *J. Am. Chem. Soc.* **1990**, *112*, 3896.
52	de Silva, A. P.; Gunaratne, H. Q. N.; Maguire, G. E. M. *J. Chem. Soc. Chem. Commun.* **1994**, 1213.
53	de Silva, A. P.; Gunaratne, H. Q. N.; McCoy, C. P. *Nature* **1993**, *364*, 42.